INTERNAL DISRUPTIONS IN STELLARATORS*

B.A. CARRERAS, V.E. LYNCH, H. ZUSHI**, K. ICHIGUCHI†, M. WAKATANI‡
Oak Ridge National Laboratory
Oak Ridge, Tennessee 37831, U.S.A.

Abstract

Internal disruptions have been observed in different modes of stellarator operation. In Heliotron E shifted-in vacuum magnetic field configuration, the ideal modes of the $m/n = 2/1$ helicity can be unstable. Their nonlinear evolution leads to a sudden crash of the pressure within the $r/a = 0.3$ radius (sawtooth oscillation). When beta is increased further, the $q = 2$ surface moves out of the plasma, and the ideal modes of the $m/n = 2/1$ helicity are effectively stabilized when $q(0) < 1.85$. As a result, the sawtooth oscillations are suppressed.

1. INTRODUCTION

Although zero-current stellators are free from major disruptions, they are not free from internal disruptions and sawtooth oscillations. Experiments in Heliotron E [1] have shown the possibility of internal disruptions near $q = 1$ and $q = 2$. The first ones were caused by resistive pressure-gradient-driven instabilities. Sawtooth oscillations near $q = 2$ surfaces have been triggered by shifting in the magnetic axis [2]. The observations indicate that these sawtooth oscillations are possibly linked to an $m = 2$ instability. This instability is associated with the $q = 2$ surface, which is very close to the magnetic axis ($r/a \approx 0.15$) for the shifted-in vacuum magnetic field configuration [3]. The application of electron cyclotron resonance heating (ECRH) at the core suppresses the sawtooth oscillations, while increasing the pressure gradient at the radial position of the $q = 2$ vacuum magnetic field resonance surface. Results of a magnetohydrodynamic (MHD) analysis of these discharges show that the $n = 1$ ideal interchange modes are linearly unstable for the sawtoothing discharges with $m = 2$ being the dominant one. The increase in peak beta associated with the ECRH causes a stabilization effect near the magnetic axis and finally even removes the $q = 2$ surface from the plasma. The ideal $m = 2$ becomes stable when $q(0) < 1.85$. The suppression of the sawtooth oscillations is probably caused by the stabilization of the ideal interchange modes.

When the ideal modes are linearly unstable, the nonlinear evolution leads to an $m = 2$ magnetic reconnection across the magnetic axis in the way suggested by Kadomtsev [4]. This causes a sudden reduction of the central pressure and a sawtooth oscillation. This nonlinear behavior is similar to the experimental results for sawtoothing discharges. For equilibrium stable to ideal interchange, the evolution of the resistive interchange leads to nonlinear saturation of the instability to a relatively low fluctuation level. These results indicate that the resistive interchange mode cannot be the cause of the sawtooth oscillations. Therefore, the sudden triggering of the instability is the consequence of the local pressure gradient going above the threshold value for the ideal interchange instability.

2. LINEAR STABILITY ANALYSIS OF HELIOTRON E DISCHARGES

To reconstruct a zero-current equilibrium, we need to know only the pressure profile. The central region of the profiles in Fig. 1 can be fitted with a function of the form $p = P_0(1-\psi)^{\alpha}$. We have found good fits with $\alpha = 4.5$ for the discharge without ECRH and $\alpha = 10.0$ for the one with ECRH. Here ψ is the poloidal flux function normalized to the plasma edge value. Using the averaging method approach [5], equilibrium sequences with varying beta have been calculated for each of the pressure profiles. The Shafranov shift modifies the rotational transform and magnetic field curvature near the $q = 2$ vacuum

*Research sponsored by the Office of Fusion Energy, U.S. Department of Energy, under contract DE-AC05-96OR22464 with Lockheed Martin Energy Research Corporation.
**Research Institute for Applied Mechanics, Kyushu University, Kasuga 816, Japan
†National Institute for Fusion Science, Toki 509-5292, Japan
‡Graduate School of Energy Science, Kyoto University, Kyoto, Japan

magnetic surface even for relatively low values of beta. The change is such that the $q = 2$ leaves the plasma at about $\beta(0) \approx 0.9\%$ for the $\alpha = 10$ profile and at about $\beta(0) \approx 0.7\%$ for the one with $\alpha = 4.5$.

We have used pressure profiles with $\alpha = 4.5$ and $\alpha = 10.0$ to reconstruct the equilibrium with the VMEC code. To study the linear ideal stability properties, we have used the RESORM code [6] based on the averaged method. The results of the calculations for the two sequences of equilibria with fixed profile and varying $\beta(0)$ are shown in Fig. 1. There is a clear instability threshold for $\beta(0) \approx 0.12\%$ for the $\alpha = 4.5$ profile and at about $\beta(0) \approx 0.08\%$ for the one with $\alpha = 10$. The linear growth rates rise sharply to values of the order of $\gamma \approx 0.01(1/\tau_{Hp}) \approx 3\times10^4\ s^{-1}$; that is, $\gamma^{-1} \approx 30\,\mu s$. In Fig. 1, the open circles and open squares indicate that the instability is a resonant $m = 2$ interchange mode. This is the dominant instability above the ideal threshold and up to beta values of $\beta(0) \approx 0.5\%$ for the $\alpha = 4.5$ profile and $\beta(0) \approx 0.3\%$ for the $\alpha = 10.0$ profile. Above these beta values, the dominant instability becomes nonresonant. Similar nonresonant instabilities of resistive character that are localized near the magnetic axis have already been identified for Heliotron E type equilibria [7]. The nonresonant instabilities dominate even when the magnetic axis transform decreases below 0.5. Finally, the equilibria are stable to $n = 1$ ideal modes for $\beta(0) > 1.1\%$ for the $\alpha = 4.5$ profile and $\beta(0) > 1.5\%$ for the $\alpha = 10.0$ profile. These results are not completely consistent with the experimental results in the following sense. The discharge without ECRH [$\alpha = 4.5$; $\beta(0) > 0.8\%$] has clear MHD activity, consistent with the linear stability results, but no activity is present for the one with ECRH [$\alpha = 10.0$, $\beta(0) > 1.2\%$], which is also linearly unstable. However, the value of $\beta(0)$ at which the nonresonant modes are stabilized is very sensitive to $q(0)$ and details of the pressure profile. Therefore, the lack of MHD activity for the ECRH discharges is possibly due to the stabilization of this mode.

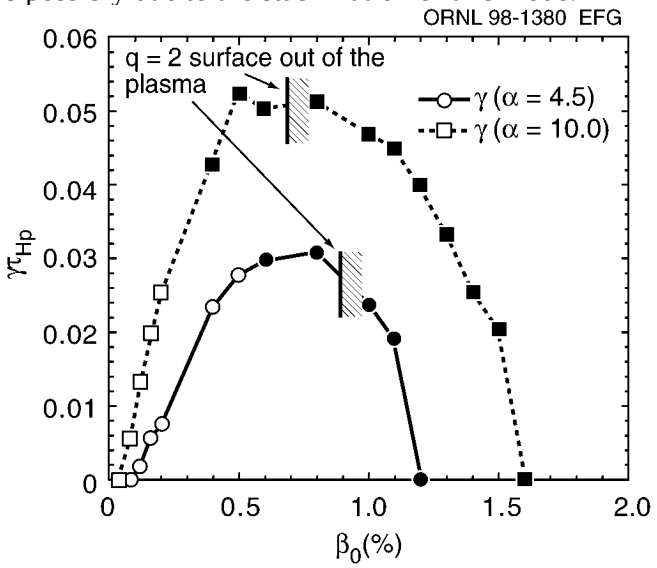

FIG. 1. Linear growth rate for two sequences of equilibria with pressure profiles with $\alpha = 4.5$ and $\alpha = 10.0$, respectively. The open circles and open squares indicate that the instability is a resonant $m = 2$ interchange mode. The full circles and full squares indicate that the instability is a nonresonant $m = 2$ mode.

3. NONLINEAR EVOLUTION OF IDEAL INTERCHANGE MODES

Nonlinear calculations have been carried out using the reduced MHD equation for stellarator configurations [8]. They have been done for equilibria corresponding to the two profiles discussed in previous sections. The Lunquist number, $S \equiv \tau_R/\tau_{HP}$, is $S = 2.1 \times 10^5$ for the ECRH on discharge and $S = 0.9 \times 10^6$ for the ECRH off. Here, $\tau_R \equiv a^2\mu_0/\eta(0)$ is the resistive time, and $\tau_{HP} \equiv R_0\sqrt{\mu_0\rho_m/B_0}$ is the poloidal Alfvén time. We have used diffusivity

coefficients for the fluctuating quantities: $D = 0.1\ a^2/\tau_R$, and $\mu = 0.1\ a^2/\tau_R$. They are chosen to control the spectrum of modes used in the calculation. For the averaged pressure evolution, $D_0 = 1.0\ a^2/\tau_R = 0.4\ m^2/s$. From the linear stability analysis in the parameter range of the experiments, we have found three types of instabilities that are relevant: resistive interchange, ideal interchange, and ideal nonresonant instabilities.

We consider an equilibrium with $\beta(0) = 0.4\%$, the $\alpha = 4.5$ pressure profile, and $q(0) = 2.1$. For this equilibrium, several modes in the 2/1 helicity are unstable, and they are ideal interchange instabilities. The nonlinear evolution shows the fast increase of X-ray emissivity ($\Delta I/I$), on the time scale of the inverse linear growth rate (about 30 μs). This is followed by a fast crash (about 10 μs) of $\Delta I/I$ and the central pressure. The central hot spot splits in two, and both move outward. To see the relaxation oscillations, we have redone the calculation with a source term in the pressure evolution equation. After a transient phase, the evolution leads to the sequence of sawtooth oscillation.

After the sawtooth collapse, the pressure gradient at the $q = 2$ surface first reverses, then turns back to negative, and slowly builds up. During the whole evolution, the local pressure gradient never reaches the value that it had initially, $dp_{eq}/dr = -1.4$. Its most negative value at the $q = 2$ surface, just before the ideal mode is triggered, is about $dp_{eq}/dr = -0.5$. If we look at the fluctuation level during this phase of the evolution, we see a nearly constant steady-state level. This fluctuation level probably corresponds to the saturation level of the resistive interchange mode below the ideal threshold. The onset of the ideal mode is very fast, causing the next sawtooth crash. In looking at the individual components of the poloidal magnetic flux at the resonance surface, we see that the steady-state phase is dominated by the ($m = 2$; $n = 1$) component, while the fast growth seems to be caused by only the ($m = 4$; $n = 2$) component. However, this is misleading because the $m = 2$ component, essentially being driven by an ideal instability, is practically zero at $r = r_s$, while the $m = 4$ component, being dominantly a resistive interchange, is nonzero.

To better understand the detailed dynamics of the evolution, we have plotted contours of the helical flux function at four different times in the evolution (Fig. 2). Before reaching the threshold of the ideal instability, there is a set of four magnetic islands at the resonant surface. They are really a combination of $m = 2$ and $m = 4$ magnetic components, with the $m = 2$ being the dominant one. Just above the threshold, a strong $m = 2$ deformation of the magnetic flux surface grows; it compresses the plasma core (from the top and bottom) until the helical flux reconnects through the magnetic axis, expelling two flux tubes on the left and right. This expulsion of flux causes the hot spots to move to $r/a \approx 0.26$ outside the "old" $q = 2$ surface $r/a \approx 0.195$. A similar effect is observed in the experiment. After the reconnection, the magnetic configuration relaxes to a state similar to the initial state. The reconnection process is very similar to the one described by Kadomtsev [4]. The only difference is the existence of the $m = 4$ islands being coupled to the process.

The last type of instability to consider is the nonresonant ideal mode. To investigate the dynamics of the nonlinear evolution, we have considered two plasma equilibria with $q(0) = 1.923$ and $q(0) = 1.85$, respectively. In either case, there is no $q = 2$ surface in the plasma. The linear growth rate of the $m = 2$ mode is close to the value for the resonant mode. The nonlinear evolution looks similar to the resonant case. However, for $q(0) = 1.85$, the effect of the instability is rather weak. An important difference between the resonant and nonresonant instability is in the magnetic reconnection process. In the present case there are no magnetic islands in the initial growth phase because there is no resonant surface in the plasma. The reconnection is a pure ideal $m = 2$ driven reconnection. The modification of the q profile by the reconnection brings in the $q = 2$ surface. However, there is no process back to axisymmetry. When a heating source has been introduced, no repetitive sawtoothing has been produced in the case of the nonresonant instability. Therefore, although the linear growth rates are similar between resonant and nonresonant instabilities, the nonlinear behavior is different. For practical purposes, the sawtooth activity is suppressed when the $q = 2$ surface is out of the plasma.

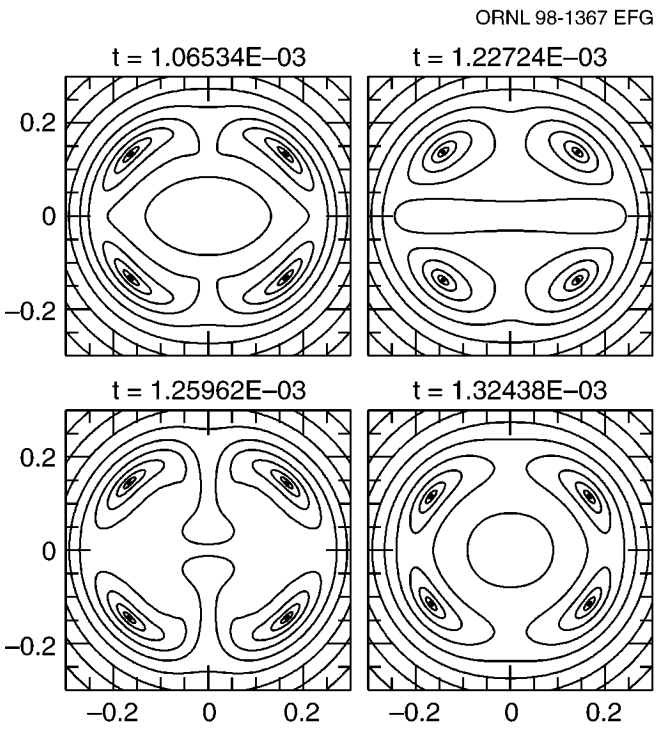

FIG. 2. Contours of the helical flux function at four different times during a full sawtooth.

4. DISCUSSION AND CONCLUSIONS

An ideal instability seems to be a likely mechanism that explains the sawtooth oscillations observed in Heliotron E plasmas with a shifted-in vacuum magnetic field axis. Depending on the beta value, this instability is an ideal interchange mode or an ideal non - resonant instability near the magnetic axis. The nonlinear evolution of 2/1 helicity for either instability reproduces the following features of the experiment:

(1) A sudden increase of the fluctuations in the precrash phase when the averaged pressure gradient is only slowly evolving. This is caused by crossing the ideal instability threshold of the interchange mode.
(2) The sawtooth crash through a magnetic reconnection across the magnetic axis.
(3) The outward expulsion of two flux tubes, which causes a double hot spot to move outside the initial $q = 2$ surface.
(4) In the case of a resonant mode, a steady-state fluctuation is induced by the resistive branch of the instability, which is responsible for the m=2 oscillations observed before and after the sawtooth crash.

Furthermore, for zero-current equilibria when $\beta(0) > 1.5\%$, the $q = 2$ surface is out of the plasma, and the equilibrium is stable to ideal modes. This finite beta effect may explain the suppression of the sawtooth oscillations when ECRH is added to a Heliotron E sawtoothing plasma.

References

[1] UO, K., Nucl. Fusion **25,** 1243-1248 (1985).
[2] ZUSHI, H., et al., in Proceedings of the 16th IAEA Fusion Energy Conference, (International Atomic Energy Agency, Vienna, 1996).
[3] WAKATANI, M., et al., in Plasma Physics and Controlled Nuclear Fusion Research, Vol. 2, (International Atomic Energy Agency, Vienna, 1991), pp. 567-575.
[4] KADOMTSEV, B.B., in Plasma Physics and Controlled Nuclear Fusion Research 1976, Vol. 1 (International Atomic Energy Agency, Vienna, 1977), pp. 555-565.
[5] GREENE, J.M., and JOHNSON, J. L., Phys. Fluids **4,** 875-890 (1961).
[6] ICHIGUCHI, K., et al., Nucl. Fusion **29,** 2093-2105 (1989).
[7] ICHIGUCHI, K., et al., Nucl. Fusion **31,** 2073-2085 (1991).
[8] CARRERAS, B.A., et al., Phys. Plasmas **3,** 2903-2911 (1996).